Academic Journal of Emerging Technologies
ISSN Print: 3104-4417
ISSN Online: 3104-4425
CD ISSN: 3104-4433
https://doi.org/10.63313/AJET.9024

Research on the Measurement of Intermediate Mass Fragments Based on a Silicon Telescope System

Kun Yang. Xiangjun Liao*
Minzu Normal University of Xingyi, Xingyi 562400, China
Email: yangkun@xynun.edu.cn

How to cite this paper: Yang, K., & Liao, X. J. (2025). Research on the Measurement of Intermediate Mass Fragments Based on a Silicon Telescope System. *Academic Journal of Emerging Technologies*, 2(1), 1–9. Print ISSN: 3104-4417; Online ISSN: 3104-4425.
https://doi.org/10.63313/AJET.9024
Published: 2025-12-11

Abstract

Intermediate Mass Fragments (IMFs) produced in heavy-ion collisions at Fermi energies are crucial observables for investigating reaction mechanisms, nuclear matter properties, and multifragmentation dynamics. Their production is closely related to the nuclear equation of state, liquid-gas phase transition, and the compression-epansion process of excited nuclear matter. Reliable measurements of IMF charge, mass, energy, and angular distributions are essential for understanding the thermodynamic evolution and dynamical behavior of nuclear systems under intermediate-energy collisions. In this study, a multi-layer silicon telescope system composed of four silicon detectors and a CsI(Tl) scintillator was employed to measure IMFs emitted from the 40 AMeV ^{64}Zn + ^{112}Sn reaction. Positioned at 20° relative to the beam direction, the telescope covers two angular ranges and provides adequate solid-angle coverage for fragments detection.

Clear ΔE-E correlation spectra were obtained, enabling isotopic identification from He (Z = 2) up to Ca (Z = 20). Up to 6-8 isotopic lines were resolved for each element, demonstrating excellent particle identification and energy resolution. After detector calibration and linearization, energy spectra and fragment yields were extracted. The experimental data exhibit characteristic multifragmentation features commonly observed in the Fermi-energy domain. The obtained IMF distributions provide meaningful constraints for nuclear reaction models and transport simulations.

This work demonstrates the capability of the Si-CsI telescope system for IMF measurements and provides a robust experimental foundation for future studies of reaction mechanisms, thermal properties of nuclear matter, and isotopic scaling behaviors in intermediate-energy heavy-ion collisions.

Keywords

Intermediate Mass Fragments; heavy-ion collisions; silicon telescope; ΔE-E particle identification

1. Introduction

In the Fermi energy region of 30-50 AMeV, heavy-ion collisions exhibit complex and diverse dynamical processes, including deep inelastic scattering, pre-equilibrium emission, collective compression-expansion dynamics, and may also involve non-trial phenomena such as nuclear liquid-gas phase transition and multifragmentation [1-3]. In this energy region, the incident heavy ions possess sufficient kinetic energy to cause significant heating and deformation of nuclear matter, but not enough to completely destroy the nuclear structure, resulting in the system's evolution being governed by the combined effects of nuclear force, Coulomb force, and many-body dynamics. The production of Intermediate Mass Fragments (IMFs, $3 \leq Z \leq 20$) is a direct reflection of these complex mechanisms, making them important subjects for experimental and theoretical research in nuclear physics [4].

The formation process of IMFs can reflect the thermodynamic behavior of nuclear matter in the low to medium density region. Especially in neutron-proton asymmetric nuclear reactions, their isotopic abundances and energy distributions provide key constraints for studying the symmetry energy term and its density dependence [5-7]. In decades of research, IMF yields have been widely used to investigate the soft/hard nature of the nuclear matter Equation of State (EOS), the conditions for the onset of nuclear liquid-gas phase separation, and the validation of transport models such as AMD, QMD, BUU [8-11]. By precisely measuring IMF distributions under different incident energies, system sizes, and isotopic compositions, important experimental evidence can be provided for the thermodynamic and dynamic transport properties of nuclear matter.

At the experimental level, the precise detection of IMFs presents significant challenges. On one hand, reactions in the Fermi energy domain involve numerous particle species with a large energy span, ranging from a few MeV/u to hundreds of MeV/u; on the other hand, the identification of heavy ion fragments' Z and A imposes stringent requirements on the detector system, necessitating high energy resolution, a large dynamic range, and sufficient geometric coverage simultaneously. The $\Delta E - E$ telescope system based on silicon detectors and CsI(Tl) scintillators has become the standard technique in IMF measurements owing to its well-defined energy-loss behavior and high particle-identification performance [12–14].

The telescope system used in this study consists of four silicon detectors of different thicknesses and one CsI(Tl) crystal, enabling reliable discrimination from light charged particles (LCPs) to intermediate mass fragments. The device is installed at an angle of 20° relative to the beam direction, covering two small angular regions, allowing the detection of a large number of forward-emitted IMFs. By correlating the energy loss (ΔE) with the residual energy (E), clear two-dimensional spectra can be obtained, enabling the identification of different nuclides and their isotopes. Furthermore, through multi-point calibration and linearization of the detectors, the energy spectra and angular distributions of the fragments can be obtained, providing essential data for analyzing reaction mechanisms [15].

Although large detector arrays such as INDRA, CHIMERA, and FAZIA have been widely used for IMF studies in recent years, medium-sized silicon–CsI telescope systems still play an important role. Their simple structure, excellent energy resolution, and low noise make them suitable for precision studies, validation experiments, and model benchmarking [16]. Furthermore, obtaining high-quality IMF data with smaller systems reduces experimental cost while allowing better control of systematic uncertainties.

This work aims to systematically analyze the production of IMFs, particle identification capability, two-dimensional energy spectrum structure, and yield patterns based on the constructed Si-CsI multilayer telescope system. Through in-depth discussion of the experimental data, it hopes to provide a reliable reference for further research on IMF dynamics, improving detector system performance, and exploring the nuclear matter equation of state.

2. Theoretical Basis and Experimental Principle

In the study of heavy-ion nuclear reactions at intermediate energies, accurately identifying the particle type, kinetic energy, and isotopic composition of reaction products is an essential foundation for understanding nuclear reaction mechanisms and the properties of nuclear matter. The development of experimental physics has shown that by utilizing the laws of energy loss of particles in matter, different nuclides and isotopes can be distinguished with high precision. The ΔE-E telescope system, composed of silicon detectors and cesium iodide scintillators, is designed based on this principle to achieve particle identification and energy spectrum measurement. In this chapter, the discussion will proceed from four aspects: the theory of particle energy loss, the $\Delta E-E$ particle identification mechanism, the physical background of nuclear reactions in the Fermi energy region, and the theory of intermediate-mass fragment formation, serving as the theoretical basis for this experimental work.

2.1. The Bethe-Bloch Formula

When a charged particle passes through matter, it undergoes Coulomb interactions with electrons in the atoms of the medium, resulting in a loss of its kinetic energy. This energy loss rate can be accurately described by the famous Bethe-Bloch formula. Its standard form can be expressed as:

$$-\left(\frac{dE}{dx}\right)=\frac{4\pi z^2 e^4}{m_e c^2 \beta^2} nZ\left[ln\left(\frac{2m_e c^2\beta^2\gamma^2}{I}\right)-\beta^2\right] \tag{1}$$

where z represents the charge number of the incident particle, Z represents the charge number of the medium's atoms, n represents the atomic number density of the medium, I represents the mean ionization energy of the atoms, $\beta=v/c$ represents the particle's velocity relative to the speed of light, and γ represents the Lorentz factor.

The Bethe-Bloch formula reflects that the energy loss of a charged particle depends on the square of its charge and is inversely proportional to its velocity, i.e., the energy loss rate is proportional to z^2/β^2. This implies heavy fragments (high Z) experience more significant energy loss, high-velocity fragments experience relatively weaker energy loss, and particles with different Z will form distinct bands on a $\Delta E - E$ plot. This is also the physical basis for the $\Delta E -$ E identification method to clearly distinguish different particles. Furthermore, the Bethe-Bloch formula also indicates that the amount of energy loss does not directly depend on the mass A, but the particle's velocity is related to its mass. Therefore, isotopes will show slight separation on the $\Delta E - E$ plot, and for light ions (p, α) , the energy loss is small, while for intermediate-mass fragments, the energy loss is greater, making the identification of IMFs more stable. To further improve particle identification accuracy, multiple layers of silicon detectors are used in the experiment, allowing the energy loss process to be recorded in greater detail.

2.2. ΔE-E Particle Identification Principle

$\Delta E - E$ telescope is one of the most commonly used particle identification systems in heavy-ion nuclear reaction experiments. Its core principle is particles lose part of their energy when passing through the front thin silicon detector (ΔE layer), and the remaining energy is completely absorbed in the rear thick detector (E layer). Since the energy loss behavior differs for different particles, by plotting the information of ΔE and E into a two-dimensional spectrum, clearly separated bands formed by different particles can be observed. For example, He (α particles) form the band with the lowest ΔE; Li, Be, and B bands gradually shift upward; and bands of heavier particles like O, Ne, Mg, and Si are significantly higher. The reason is that the energy loss rate increases with increasing z^2, so particles with large Z lose more energy in the ΔE layer.

Within the band of particles with the same Z, clear isotopic separation also appears. This arises because different masses affect particle velocity, which in turn affects the amount of energy loss. Particles with larger mass numbers have lower velocities and slightly larger ΔE values, and differences in binding energy lead to different incident energies, causing them to form separated isotopic branches on the spectrum. Therefore, the ΔE-E identification method can distinguish both Z and, for some cases, A values. In this experiment, the ΔE-E telescope system consists of 4 Si detectors and 1 CsI detector. The ΔE layer is provided by thin silicon, and high-Z particles can be completely stopped in the rear silicon layer or CsI, enabling Z and A identification across the full energy range.

2.3. Role of CsI(Tl) scintillator in E measurement

In the process of stopping high-energy particles, silicon detectors have limited thickness and cannot fully absorb IMFs with energies of tens of MeV/u, so thicker materials must be used as supplements. In this experiment, the CsI crystals, together with the Si detectors, form a complete ΔE-E energy spectrum structure, significantly improving the resolution of the spectrum.

3. Experimental Setup and Methods

To systematically study the intermediate mass fragments produced in 40 AMeV $^{64}Zn + ^{112}Sn$ heavy-ion reactions, this study constructed a multi-layer telescope system consisting of four silicon detectors and one CsI(Tl) crystal in the Scattering Chamber, see Figure 1. This system is designed to achieve precise identification and high-resolution energy measurement of particles ranging from light charged particles (LCPs) to intermediate mass fragments (IMFs). This section will provide a comprehensive description of the entire experimental system, covering aspects such as beam conditions, target material, detector structure, electronic signal processing, trigger logic, and data acquisition system (DAQ), laying a solid foundation for the presentation and analysis of subsequent experimental results.

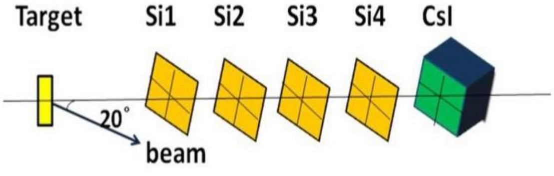

Figure 1. Schematic diagram of the silicon telescope system

3.1. Beam Conditions and Target Material

The beam used in the experiment was: a ^{64}Zn heavy-ion beam, with an energy of 40 AMeV, a beam intensity maintained at the level of a few nA, and a beam spot size of approximately $5\ mm \times 5\ mm$. This energy region belongs to the typical Fermi energy domain, which can effectively excite incomplete fusion reactions and thereby produce a large number of intermediate mass fragments.
The experimental target nucleus was a 112Sn solid target, with a thickness of about $1mg/cm^2$, using high-purity evaporated film material and a foil backing structure to ensure thickness uniformity better than $\pm3\%$.

3.2. Structural Design of the Si-CsI Multi-layer Telescope System The telescope

The Si–CsI multi-layer telescope system consists of five detector layers. The first thin silicon layer (129 μm) provides high-resolution initial energy-loss (ΔE) measurements, enabling light charged-particle and isotope identification. The second silicon layer (300 μm) supplies additional ΔE information, contributes to stopping light fragments, and serves as the core of the trigger logic to distinguish penetrating from fully stopped events. The third and fourth thick silicon layers (each 1000 μm) stop intermediate-mass fragments (IMFs) in the 5–20 MeV/u range, extend the dynamic range, and improve energy-measurement accuracy for higher-Z particles through joint energy reconstruction with the CsI crystal. The final CsI(Tl) layer (several centimeters thick) absorbs the remaining particle energy and provides the total energy (E) signal for ΔE–E particle identification. All silicon detectors are divided into four quadrants, each covering 5° of solid angle, enabling detection at 17.5° ± 2.5° and 22.5° ± 2.5° within the forward IMF emission region, thus ensuring representative IMF statistics.

3.3. Electronics Signal Processing System

Instantaneous detection signals need to undergo a series of electronic processes to be effectively digitized and recorded. The electronics system for this experiment includes modules for pre-amplification, signal splitting, discrimination, trigger logic shaping, and timing recording, see Figure 2.

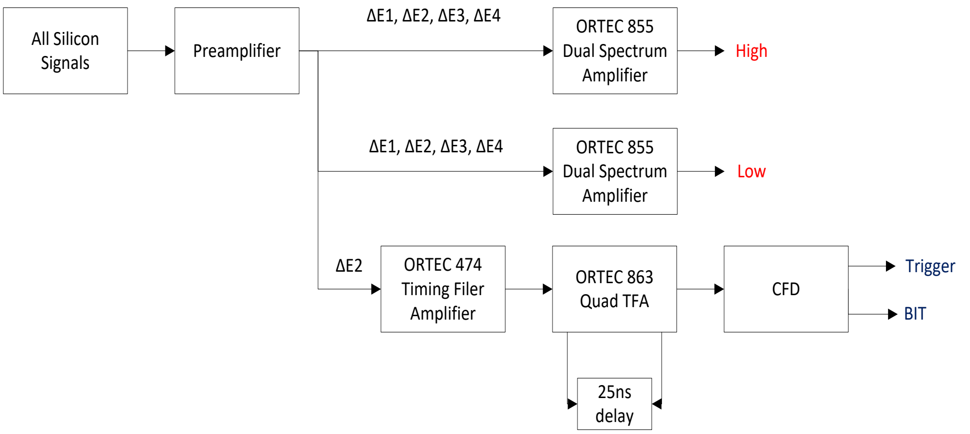

Figure 2. Block diagram of the silicon detector electronics circuitry

3.4. Data Acquisition System (DAQ)

This experiment uses a data acquisition system based on VME or NIM architecture, with the following main features: Analog-to-Digital Converters (ADC) for digitizing energy signals, Time-to-Digital Converters (TDC) for measuring time differences between signals, a Multi-Event Buffer (MEB) to prevent data loss due to dead time, and Run Control software to manage the data acquisition process. The average event rate of the DAQ system is approximately several tens to one hundred events per second, ensuring data stability during long-term operation.

4. Experimental Results

Figure 3. shows one of the most important data structures from the experiment—the ΔE-E two-dimensional correlation plot. This spectrum uses the energy loss in the second-layer silicon detector as the vertical axis and the deposited energy in the third-layer silicon detector as the horizontal axis, forming clearly separated curved bands. Closer observation reveals that particles with different charge numbers Z

form distinct, separate families with varying curvatures, and each family is further subdivided into multiple isotope bands corresponding to different mass numbers A.

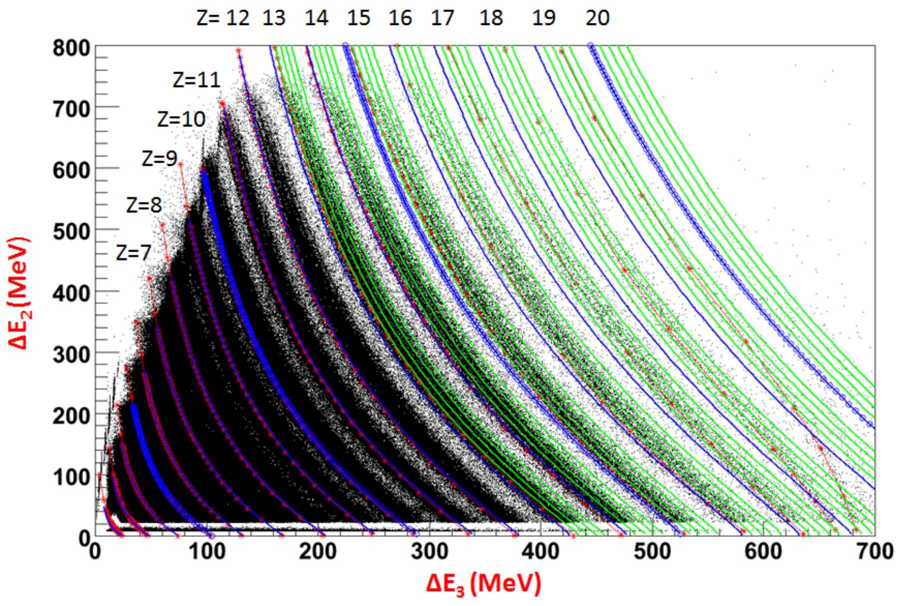

Figure 3. Two-dimensional particle energy correlation plot detected by the silicon telescope.

Due to the inherent physical properties of the $\Delta E - E$ method, the curves for light particles are relatively flat, while those for heavy particles are steeper. The shape of these bands is consistent with the energy loss of particles passing through the detector, namely the $dE/dx \propto Z^2/\beta^2$ relationship described by the Bethe-Bloch equation. Consequently, as the Z number increases, the ΔE value shows a significant increasing trend, causing the heavy fragment bands to shift noticeably upward.

All charged particle bands from He (Z=2) to Ca (Z=20) can be clearly distinguished in the two-dimensional spectrum, see Figure 4. This indicates that the multi-layer telescope system used in this experiment performs well in terms of energy coverage and resolution. Particularly for typical IMFs such as $Z = 6(C)$, $Z = 8(O)$, $Z = 12(Mg)$, $Z = 14(Si)$, the band structures are exceptionally clear, demonstrating significant separation capability.

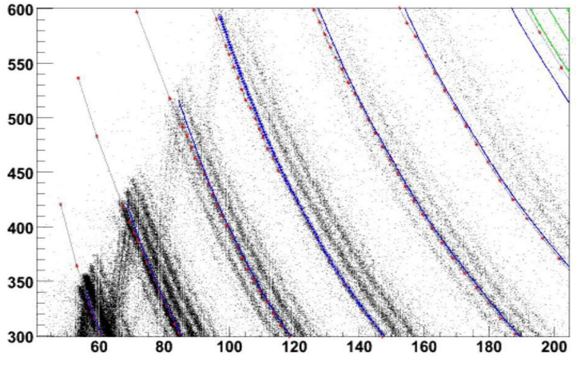

Figure 4. Magnified view of a section of the two-dimensional particle energy correlation plot

detected by the silicon telescope.

This experimental achievement is very important, as distinguishing 20 different Z particles in continuous energy-energy space is not easy and requires high synergy among multiple factors such as detector thickness, energy calibration, and noise control. Clearly, the experimental system has achieved particle identification capabilities comparable to international medium-scale array systems (such as LASSA or MUST2).

5. Conclusion

In summary, the multi-layer Si–CsI telescope system demonstrated excellent performance in identifying and characterizing intermediate mass fragments produced in 40 AMeV heavy-ion collisions. Through precise detector calibration, ΔE–E spectrum linearization, and multi-layer energy reconstruction, the system achieved clear charge and isotopic separation from light charged particles up to fragments with Z≈20, enabling the extraction of reliable energy spectra, angular distributions, and yield systematics. The observed IMF distributions, forward-focused emission patterns, and isotopic trends are consistent with the multifragmentation dynamics expected in the Fermi-energy domain and provide meaningful constraints for transport-model simulations and studies of the nuclear equation of state. Overall, this work confirms the capability and scientific value of medium-scale silicon telescope systems in nuclear reaction research and establishes a solid experimental foundation for future investigations into isospin physics, symmetry energy behavior, and the thermodynamic properties of hot nuclear matter.

Acknowledgements

Natural Science Research Support Project of Education Department of Guizhou Province (No. [2024] 350, and KY [2018] 006).

References

[1] Borderie, B., and Rivet, M. F. (2008). Nuclear multifragmentation and phase transition for hot nuclei. Progress in Particle and Nuclear Physics, 61(2), 551-601. https://doi.org/10.1016/j.ppnp.2008.01.003

[2] Chomaz, P., Colonna, M., and Randrup, J. (2004). Nuclear spinodal fragmentation. Physics Reports, 389(5-6), 263-440. https://doi.org/10.1016/j.physrep.2003.09.006

[3] Gross, D. H. E. (1990). Statistical decay of very hot nuclei-the production of large clusters. Reports on Progress in Physics, 53(5), 605. https://doi.org/10.1088/0034-4885/53/5/003

[4] Ogilvie, C. A., Adloff, J. C., Begemann-Blaich, M., Bouissou, P., Hubele, J., Imme, G., ... and Tucholski, A. (1991). Rise and fall of multifragment emission. Physical review letters, 67(10), 1214. https://doi.org/10.1103/PhysRevLett.67.1214

[5] Tsang, M. B., Friedman, W. A., Gelbke, C. K., Lynch, W. G., Verde, G., and Xu, H. S. (2001). Isotopic scaling in nuclear reactions. Physical Review Letters, 86(22), 5023. https://doi.org/10.1103/PhysRevLett.86.5023

[6] Shetty, D. V., Yennello, S. J., and Souliotis, G. A. (2007). Density dependence of the symmetry energy and the nuclear equation of state: A dynamical and statistical model per-

spective. Physical Review C, 76(2), 024606. https://doi.org/10.1103/PhysRevC.76.024606

[7] Ono, A., and Horiuchi, H. (2004). Antisymmetrized molecular dynamics for heavy ion collisions. Progress in Particle and Nuclear Physics, 53(2), 501-581. https://doi.org/10.1016/j.ppnp.2004.05.002

[8] Ono, A., Horiuchi, H., Maruyama, T., and Ohnishi, A. (1992). Antisymmetrized version of molecular dynamics with two-nucleon collisions and its application to heavy ion reactions. Progress of theoretical physics, 87(5), 1185-1206. https://doi.org/10.1143/ptp/87.5.1185

[9] Aichelin, J. (1991). "Quantum" molecular dynamics—a dynamical microscopic n-body approach to investigate fragment formation and the nuclear equation of state in heavy ion collisions. Physics Reports, 202(5-6), 233-360. https://doi.org/10.1016/0370-1573(91)90094-3

[10] Bertsch, G. F., and Gupta, S. D. (1988). A guide to microscopic models for intermediate energy heavy ion collisions. Physics Reports, 160(4), 189-233. https://doi.org/10.1016/0370-1573(88)90170-6

[11] Li, B. A., Chen, L. W., and Ko, C. M. (2008). Recent progress and new challenges in isospin physics with heavy-ion reactions. Physics Reports, 464(4-6), 113-281. https://doi.org/10.1016/j.physrep.2008.04.005

[12] Pouthas, J. O. E. L., Borderie, B., Dayras, R., Plagnol, E., Rivet, M. F., Saint-Laurent, F., ... and Wittwer, G. (1995). INDRA, a 4π charged product detection array at GANIL. Nuclear Instruments and Methods in Physics Research Section A: Accelerators, Spectrometers, Detectors and Associated Equipment, 357(2-3), 418-442. https://doi.org/10.1016/0168-9002(94)01543-0

[13] Pagano, A. (2012). Studies of Nuclear Reactions and Time Scale with the 4π Detector CHIMERA. Nuclear Physics News, 22(1), 25-30. https://doi.org/10.1080/10619127.2011.629922

[14] FAZIA Collaboration, Upadhyaya, S., Mazurek, K., Kozik, T., Gruyer, D., Casini, G., ... and Vigilante, M. (2024). Study of quasi-projectile properties at Fermi energies in 48 Ca projectile systems. The European Physical Journal A, 60(7), 157. https://doi.org/10.1140/epja/s10050-024-01369-5

[15] Lopez, O., Pârlog, M., Borderie, B., Rivet, M. F., Lehaut, G., Tabacaru, G., ... and INDRA collaboration. (2018). Improving isotopic identification with INDRA Silicon–CsI (Tl) telescopes. Nuclear Instruments and Methods in Physics Research Section A: Accelerators, Spectrometers, Detectors and Associated Equipment, 884, 140-149. https://doi.org/10.1016/j.nima.2017.12.041

[16] Hudan, S., Chbihi, A., Frankland, J. D., Mignon, A., Wieleczko, J. P., Auger, G., ... and INDRA Collaboration. (2003). Characteristics of the fragments produced in central collisions of 129 Xe+ nat Sn from 32A to 50 A MeV. Physical Review C, 67(6), 064613. https://doi.org/10.1103/PhysRevC.67.064613